Biophysical Journal, Volume 100

Supporting Material

Elucidating the role of matrix stiffness in 3D cell migration and remodeling

Martin Ehrbar, Ana Sala, Philipp Lienemann, Anne Gret Bittermann, Simone Rizzi, Franz Weber, and Matthias Lutolf

Supplementary Information Ehrbar et *al.*

1. Measurement of viscoelastic and swelling properties of TG-PEG hydrogels

The mechanical properties of pre-swollen hydrogels were measured by frequency sweeps from 0.1 to 10 Hz. G´, G´´, and the phase angle were typically constant in the frequency range from 0.1 to 1 Hz and at higher frequencies started to increase. G´ was observed to be two orders of magnitude larger than G´´.

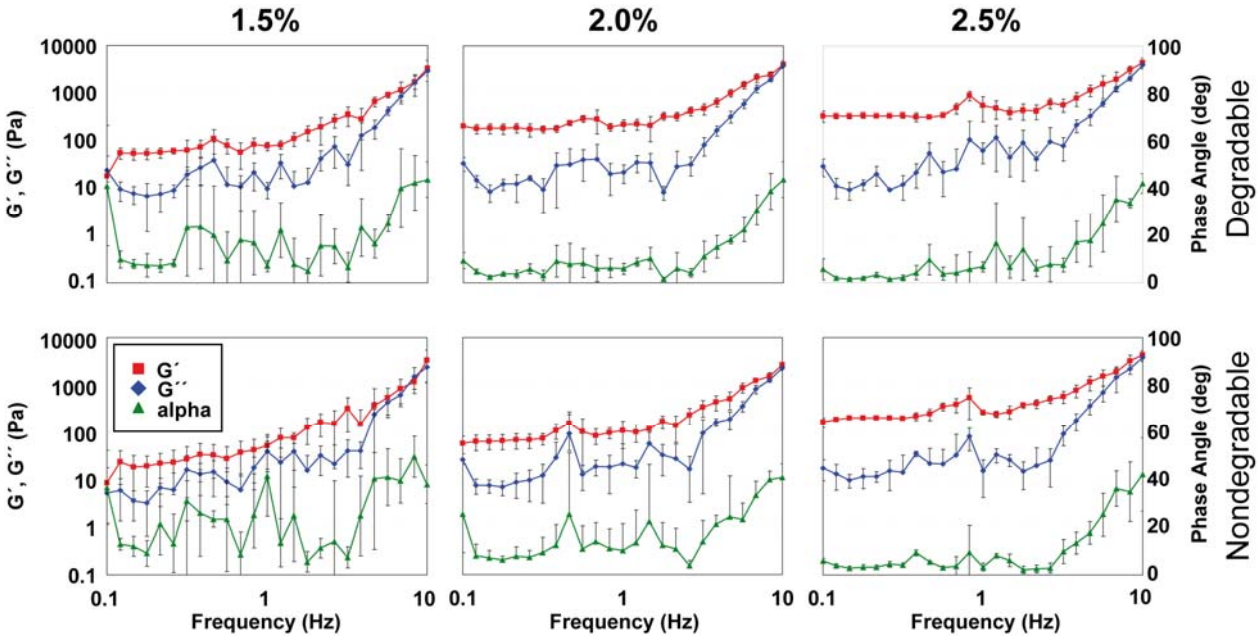

Figure S1. Typical mechanical spectra for swollen gels formed at different (w/v) precursor concentrations. G´ was constant at the low frequency range (0.1-1 Hz), and G´´ was generally around 2 orders of magnitude smaller than G´. G´´, G´ and the phase angle were seen to increase at frequencies higher than 1 Hz.

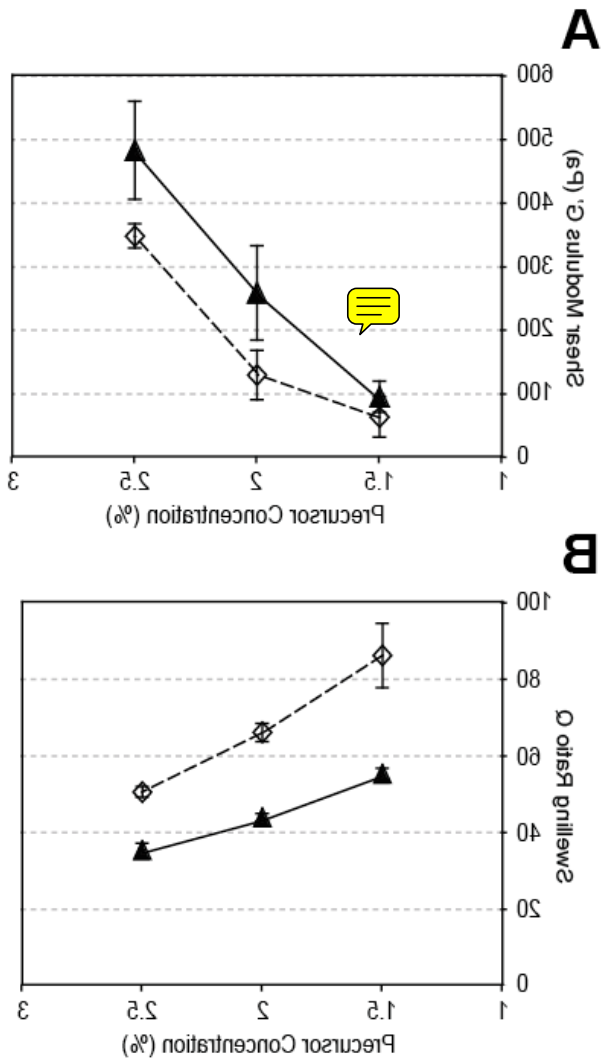

Figure S2. Physicochemical characterization of the chosen model aECMs. (**A**) The storage modulus G´ increased with increasing precursor concentration. MMP-degradable hydrogels are stiffer than MMP-insensitive gels formed at the same precursor concentration. (**B**) The swelling ratio Q decreased with increasing the precursor concentration. Notably, the MMP-insensitive hydrogels swelled consistently more than the MMP-sensitive gels. (mean ± SD, n = 5)

2. Measurement of sol fraction

The sol fraction of the gel networks formed at 1.5% was measured by RP-HPLC.

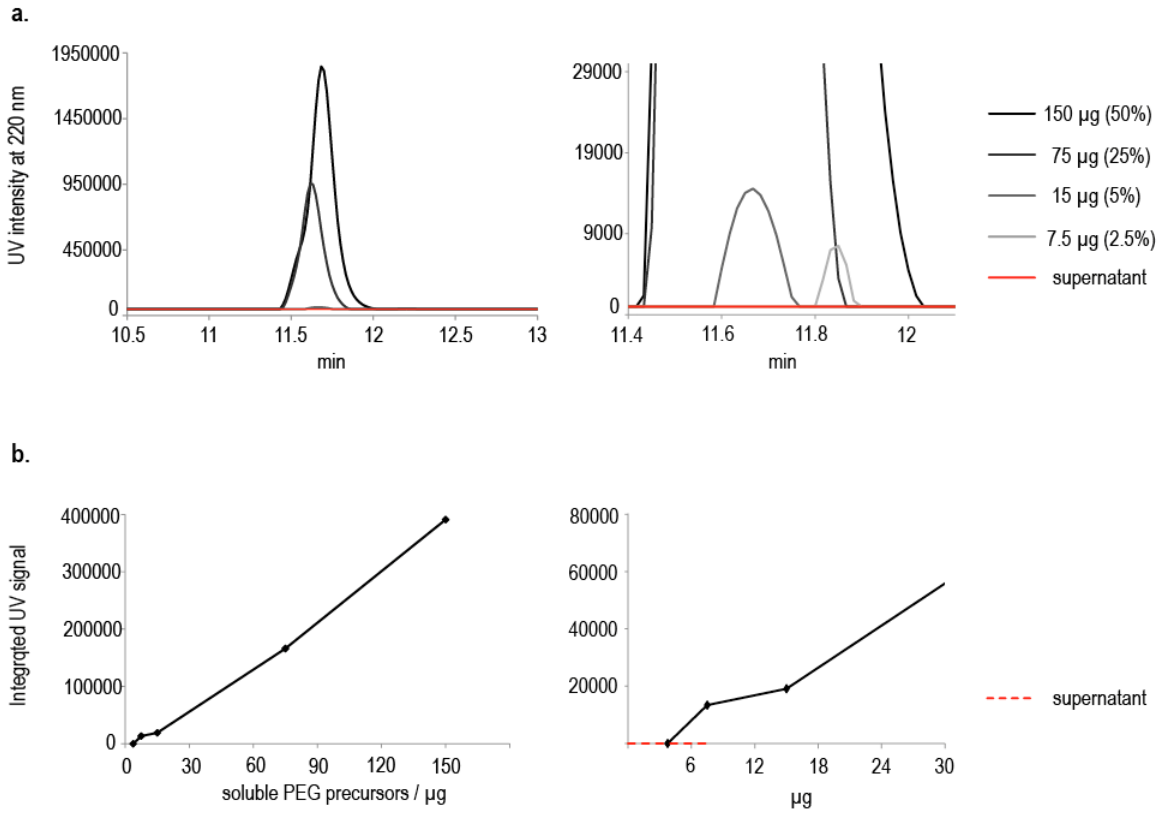

Figure S3. Evaluation of sol fraction. **(A)** chromatogram of different PEG-precursors concentrations (grey gradient) and analysis of 1.5% gel supernatant after swelling in water (ratio gel to water, 1:4) in red; **(B)** Standard curve of integrated UV signal obtained from chromatograms, showing that analyzed supernatant is below detection limits. Thus, we can afirm that any network defects would be negligible as they would be due to, at most, to 2.5% of the total gel mass remaining unreacted (and most likely less, but undetectable with our current methodology).

3. Influence of gel stiffness on 3D cell spreading

Single MC3T3-E1 murine pre-osteoblastic cells were encapsulated in degradable gels with variable stiffness and imaged by confocal microscopy after 24 hours in culture (**Fig. S4**). Cells in soft gels adapted a spindle-shaped morphology. With increasing stiffness the morphology became less elongated and reticulate filopodia were formed. In the stiff gels the cells remained almost round with frayed filopodia.

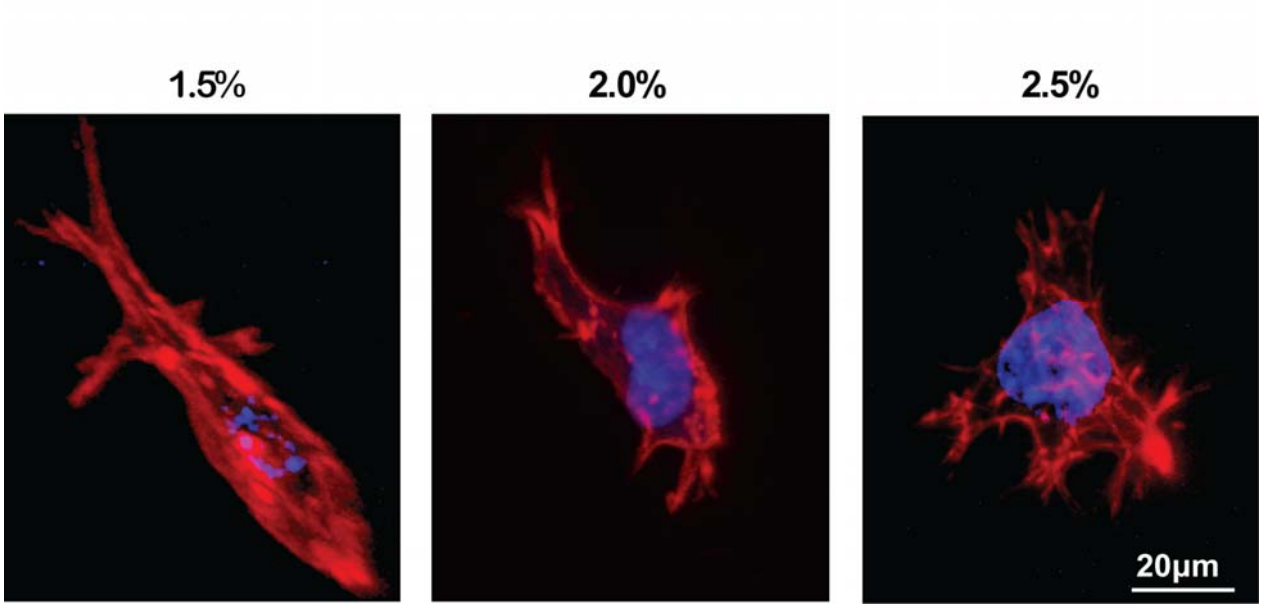

Figure S4. Typical confocal fluorescence images of spreading and elongating cells 24 hours after encapsulation of single cells in soft (1.5%), intermediate (2.0%), and stiff (2.5%) matrices. Rhodamine-phalloidin stained f-actin is shown in read and co-stained nuclei stained with DAPI are in blue.

4. The influence MMP inhibition on MC3T3-E1 cell migration

MC3T3-E1 cells were encapsulated in MMP-sensitive (**Fig. S5A**) and MMP-insensitive (**Fig. S5B**) hydrogels of different stiffness and, after initial swelling, immobilized on the bottom of tissue culture plates. In order to inhibit MMP activity, the cell culture medium was supplemented with 50 μM of the pan-MMP inhibitor GM6001. Whereas the migration of cells is blocked in intermediate and stiff MMP-sensitive gels, the migration in soft gels cannot be blocked by the inhibition of MMPs.

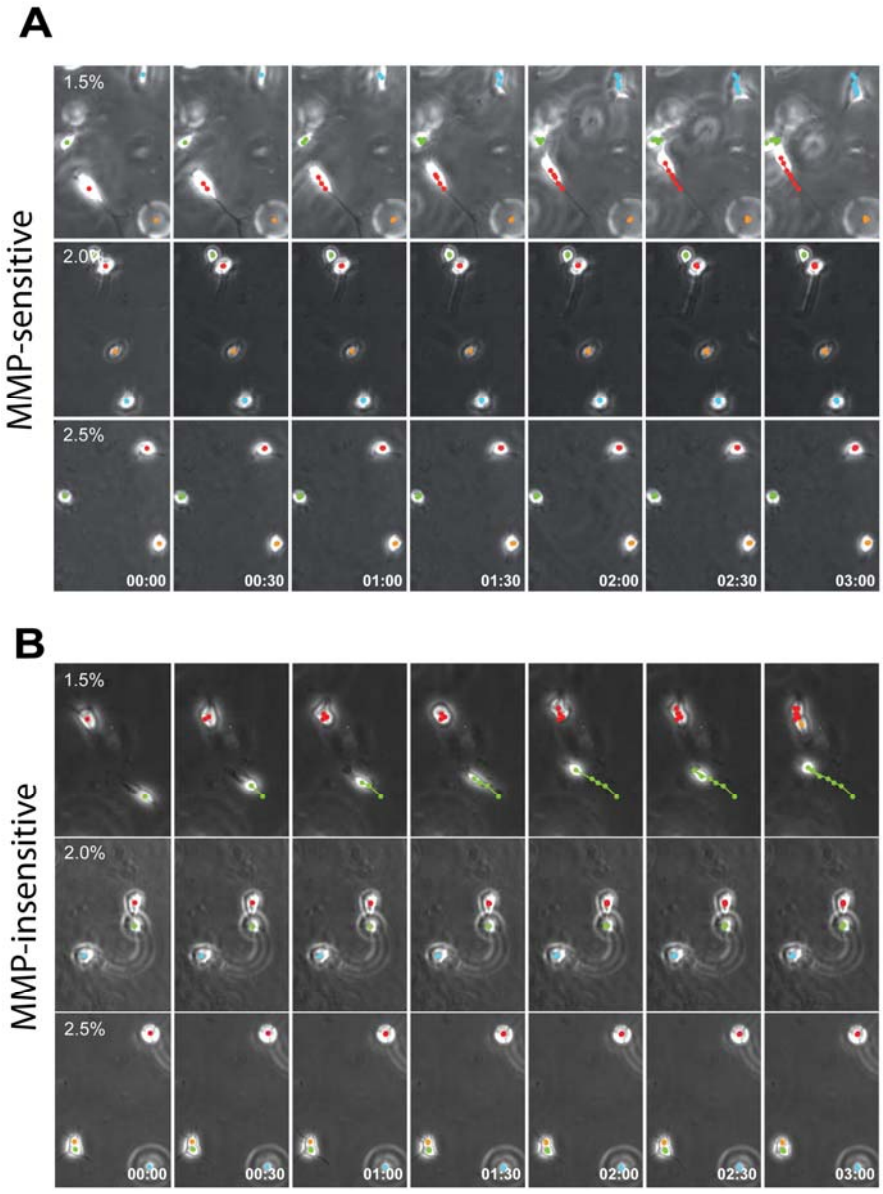

Figure S5. Representative Time-lapse images of MC3T3-E1 cells in 3D culture *in presence of MMP inhibitor GM6001* (time interval t = 30min.). Efficient migration in soft **(A)** MMP-sensitive and **(B)** MMP-insensitive hydrogels is observed, whereas the migration, but not sprout formation, is efficiently blocked by GM6001 in gels with higher stiffness.

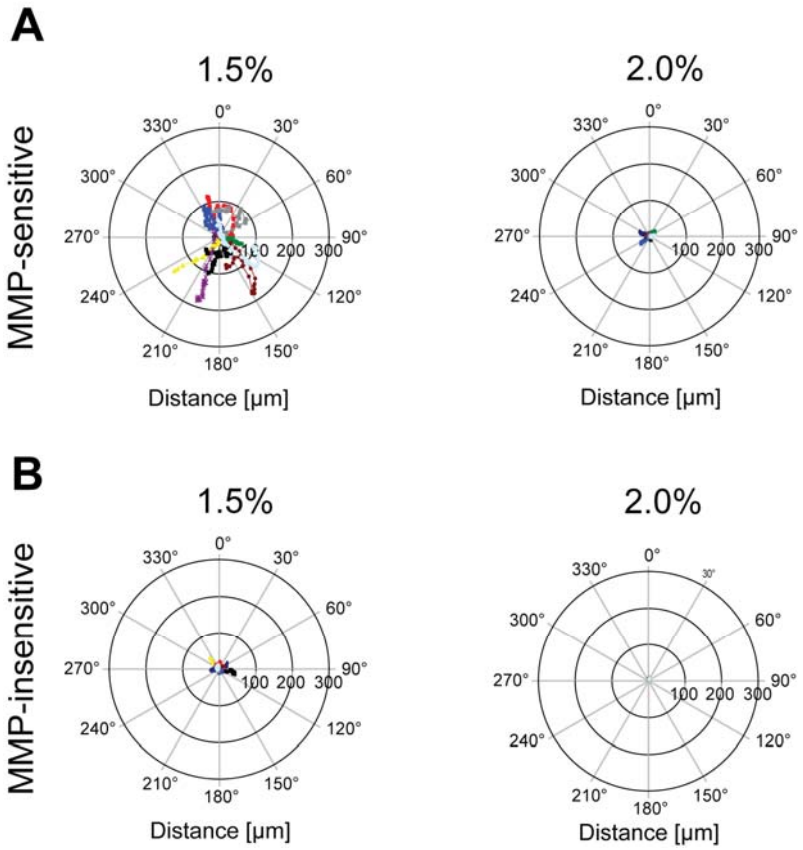

Figure S6. Representative track plots of MC3T3-E1 cells in 3D culture in presence of MMP inhibitor GM6001. The projection of 10 migrating cells was acquired and overlaid with a common starting point. The tracks representing a 14.5 hour period (58 x 15min.) do not show a preferred orientation. (**A**) Efficient migration in soft MMP-sensitive hydrogels is observed that is blocked at intermediate stiffness. (**B**) While some migration in soft MMP-insensitive hydrogels is observed the migration of cells in gels with intermediate stiffness is completely blocked by the MMP inhibitor.

5. Quantification of 3D single cell migration behavior

3D migration rate and persistence time based on time-lapse imaging series of at least 24 consecutive time frames were calculated using an unbiased random walk model (**Fig. S7**).

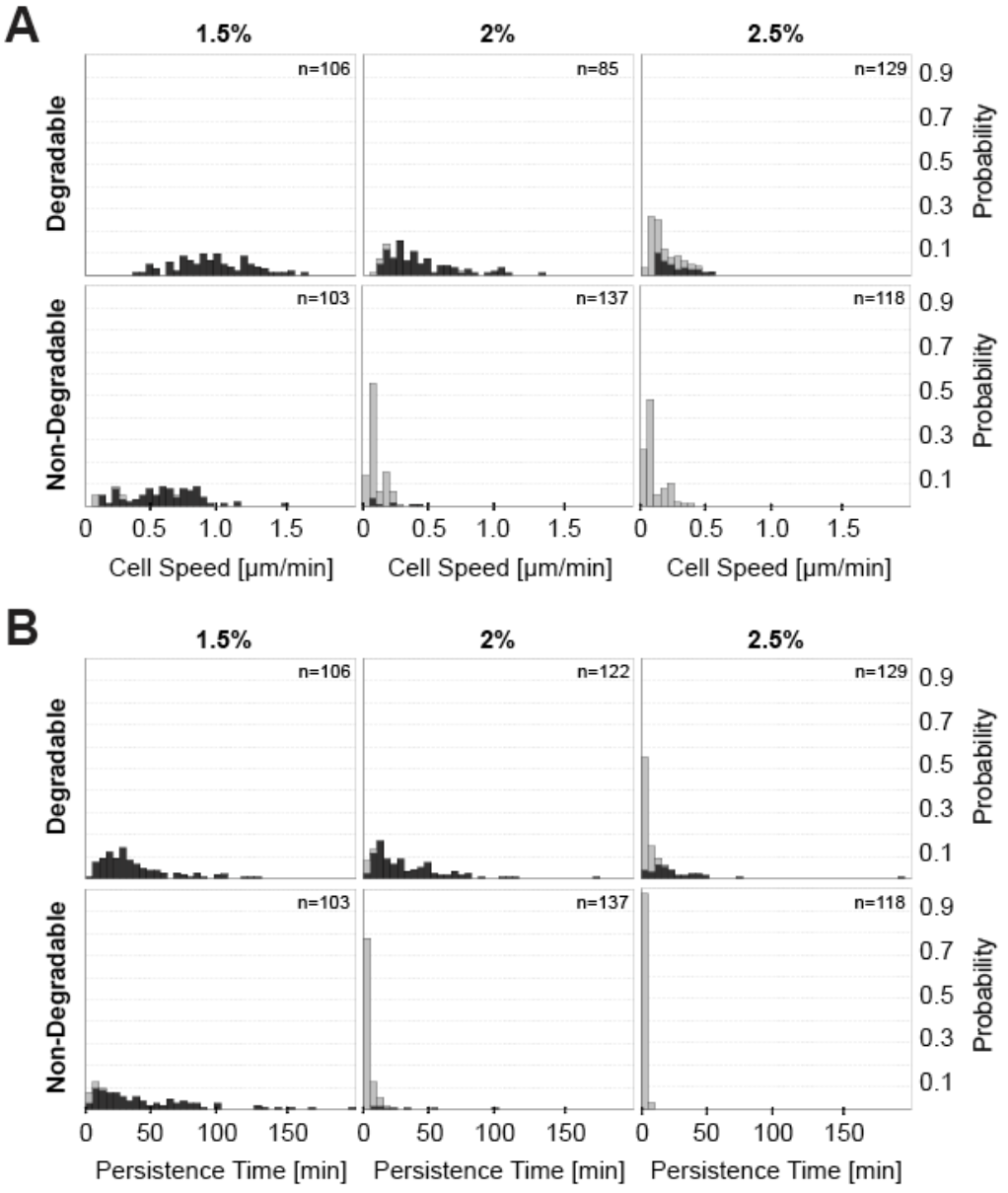

Figure S7. Migration parameters of 3D-encapsulated single cells. Cell tracks were assigned to migrating (black) or non-migrating (grey) groups, based on the persistence length criterion L_{crit}=1.2 µm. Histograms show the pooled data of three independent experiments with a total of *n* cell tracks. Depicted are **(A)** mean cell speed and **(B)** persistence time. The number of cells having a mean speed or a persistence time within a certain bin are divided by the total number of cells to give a normalized number indicated on the probability axis. Tracks with persistence time values derived from a regression analysis with R^2 <0.60 were excluded from the evaluation.

6. Determination of the migrating cell population

The percentage of migrating cells in MMP-sensitive gels decreased with increasing stiffness. (**Fig. S8**). In MMP-insensitive gels migration is only possible in soft gels and is completely blocked in intermediate and stiff gels.

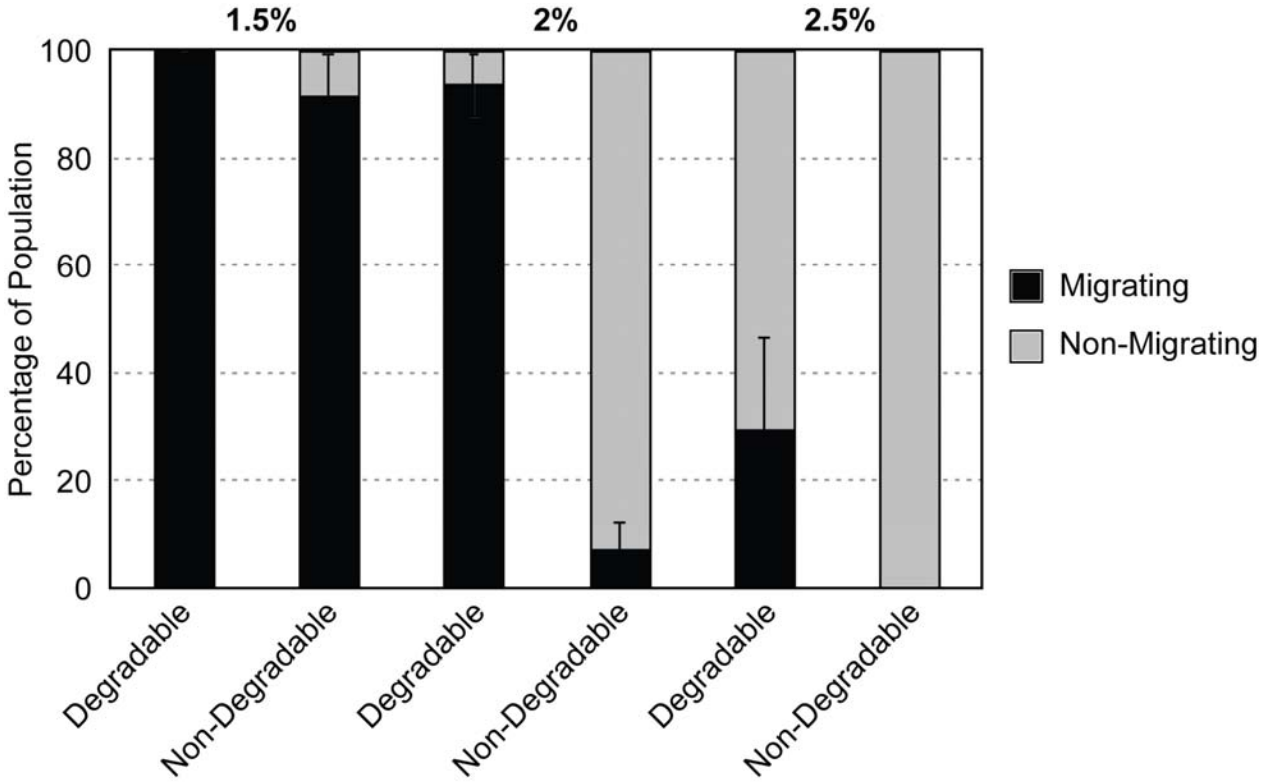

Figure S8. Migrating cell population of 3D encapsulated single-cells. Projections of 3D track were acquired with an inverse wide-field microscope and tracks were analyzed manually. After the evaluation of cell migration parameters persistence time and cell speed, cells were grouped in a migrating and non-migrating population based on the persistence length criterion L_{crit} = 1.2 μm. Each cell track was assigned to a migrating (black) or a non migrating (grey) group, based on the persistence length criterion L_{crit}=1.2 μm. All cells or almost all cell migrated in the soft gels that are MMP-sensitive or MMP-insensitive respectively. With increasing the stiffness to intermediate and stiff gels, the migrating population decreased in the MMP-sensitive gels. In the MMP-insensitive gels the migrating population was dramatically reduced in intermediate and completely absent in the stiff

7. Pan-MMP inhibitor GM6001 prevents the formation of cellular networks

Single cells cultured for three weeks in MMP-sensitive or MMP-insensitive gels form cellular networks. However migration is observed in these gels cellular network are not formed in presence of the MMP inhibitor (**Fig. S9**).

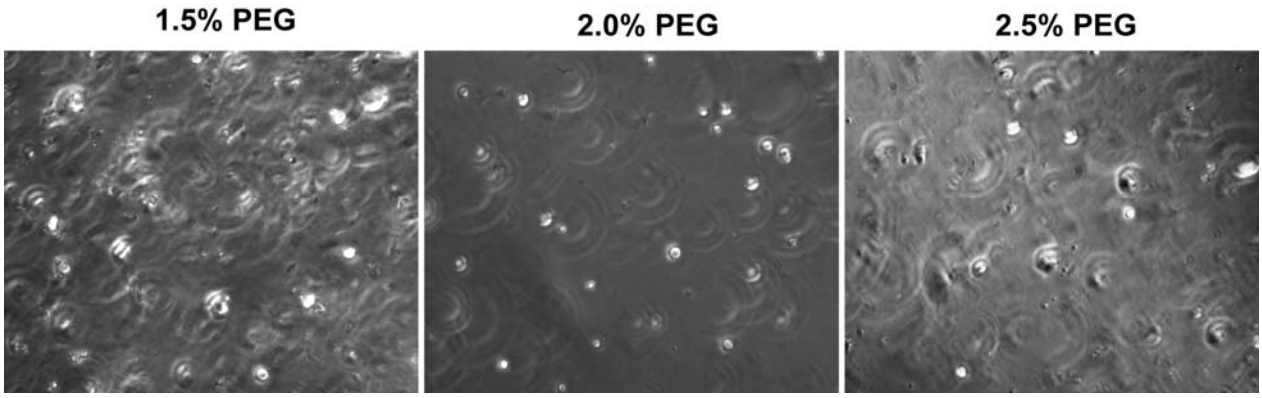

Figure S9. Cellular networks in MMP-sensitive matrices is absent in presence of MMP inhibitor. Cells that are encapsulated in soft degradable gels can migrate in presence of the MMP inhibitor GM6001. However they do not form cellular networks during the three weeks culture in presence of the inhibitor.

8. More detailed version of Materials and Methods

1.1 Material and Reagents

PEG-peptide conjugates Production and characterization of different eight-arm PEG precursors containing pending factor XIIIa substrate peptides having either a glutamine acceptor substrate (*n-PEG-Gln*) or a lysine donor substrate containing a MMP-sensitive linker (*n-PEG-MMP$_{sensitive}$-Lys)* or a MMP-insensitive linker *(n-PEG-MMP$_{insensitive}$-Lys)* was performed as described elsewhere (11). In brief, eight-arm PEG mol. wt. 40000 was purchased from Nektar (Huntsville, AL, USA). Divinyl sulfone was purchased from Aldrich (Buchs, Switzerland). PEG vinylsulfone (PEG-VS) was produced and characterized as described elsewhere (20). The factor XIIIa substrate peptides H-NQEQVSPL-ERCG-NH_2 (TG-*Gln*) Ac-FKGG-GPQGIWGQ-ERCG-NH_2 (*MMP$_{sensitive}$-Lys)* Ac-FKGG-GDQGIAGF-ERCG-NH_2 (*MMP$_{insensitive}$-Lys)*, Ac-FKGG-K-FITC (TG-*Lys-FITC)*, and the adhesion ligand Ac-GCYGRDGSPG-NH_2 (TG-*Gln-RGD*) were obtained from NeoMPS (Strasbourg, France) (immunograde, C_{18}-purified, HPLC analysis: > 90%). The NQEQVSPL cassette corresponds to the factor XIIIa substrate site in α_2-plasmin inhibitor (21), the FKGG cassette to an optimized factor XIIIa substrate site (22), and the ERCG cassette to the vinylsulfone-reactive Cysteine (23). In separate vials *TG-Gln, TG-MMP$_{sensitive}$-Lys or TG-MMP$_{insensitive}$-Lys* were added to PEG-VS in 1.2-fold molar excess over VS groups and allowed to react in 0.3 M triethanolamine (pH 8.0) at 37°C for 2 h. The products were dialyzed (Snake Skin, MWCO 10K, PIERCE, Rockford, IL, USA) against ultrapure water for 3 days at 4°C. After dialysis, the salt-free products (*8-PEG-MMP$_{sensitive}$-Lys, 8-PEG-MMP$_{insensitive}$-Lys* and *8-PEG-Gln*, respectively) were lyophilized to obtain a white powder. The peptide-PEG conjugation was confirmed via ^{1}H NMR.

1.2 PEG hydrogel preparation

100 µL of factor XIIIa (200 U/mL, a generous gift from Baxter BioSurgery, Vienna, Austria) was activated with 10 µL of thrombin (20 U/mL, Sigma-Aldrich, Switzerland) for 30 min at 37°C. Small aliquots of activated factor XIIIa were stored at -80°C for further use. Precursor solutions to give hydrogels with a final dry mass content of 1.5, 2.0 and 2.5% were prepared by stoichiometrically balanced ([*Lys*]/[*Gln*] = 1) solutions of *n-PEG-Gln* and *n-PEG-MMP$_{sensitive}$-Lys or n-PEG-MMP$_{insensitive}$-Lys* in Tris-Buffer (TBS, 50 mM, pH 7.6) containing 50 mM calcium chloride, leaving open a spare volume of 12.5% v/v for later addition of cell culture medium. The cross-linking reaction was initiated by 10 U/mL thrombin-activated factor XIIIa and vigorous mixing, immediately followed by addition of 12.5% v/v cell culture medium with or without cells. To obtain disc-shaped matrices, the liquid reaction mixtures (20 - 40 µL) were sandwiched between sterile hydrophobic glass microscopy slides (obtained by treatment with SigmaCote, Sigma) separated by spacers (ca. 1 mm thickness) and clamped with binder clips. To prevent sedimentation of cells, the forming matrices were slowly rotated for 10min. at RT (until the onset of gelation) and then incubated for additional 30min. at 37°C.

1.3 PEG hydrogel characterization

Rheometry on swollen gels. Storage and loss moduli (G' and G") of swollen gels were obtained by small strain oscillatory shear rheometry (20). Briefly, swollen hydrogel discs of 1 to 1.4 mm

thickness were sandwiched between the two plates of the rheometer with compression up to a range between 85% to 75% of their original thickness to avoid slipping. Measurements were then conducted in a constant strain (0.05) mode as a function of frequency (from 0.1 to 10 Hz) to obtain dynamic mechanical spectra (n=4 per condition).

Equilibrium swelling measurements. Swollen hydrogels were weighted just prior to rheometry, and the swelling ratio Q determined as the swollen gel mass divided by the gel's dry mass (calculated from the reaction conditions).

Detection of sol fractions by HPLC. The potential presence of defects in the network architecture due to uncrosslinked PEG precursors was investigated by reverse phase high-performance liquid chromatography (RP-HPLC). First, a dilution series of unreacted PEG precursors was run on an RP-HPLC instrument using a Waters (Milford, MA, USA) C_{18} symmetry column in order to establish a standard curve of UV intensities (recorded at 220nm) as a function of PEG concentration. Then, gels (50μl volume formed at 1.5% w/v) were prepared (n=4) and each was incubated in 200μl water for 24 hours. The supernatant was then collected, run on the HPLC instrument and UV intensities were compared to the standard curve to determine the corresponding amount of unreacted polymer remaining in solution.

1.4 Cell culture

Mouse preosteoblastic cells MC3T3-E1 were purchased from American Type Culture Collection (ATCC) and grown under in MC3T3-E1 culture medium (alpha-minimal essential medium, with 10% fetal bovine serum, 100U/ml penicillin G and 100mg/ml streptomycin GIBCO BRL, Life Technologies, Grand Island, NY, USA) under standard cell culture conditions (37°C in humidified atmosphere and 5% CO_2).

1.5 Cell encapsulation

Cells suspended in cell culture medium were added right after the FXIIIa enzyme to yield single dispersed cells at a final seeding density of 6 $x10^4$ cells / ml of hydrogel. Subsequently the forming matrices were slowly rotated (10min at RT) until the onset of gelation to prevent sedimentation of cells, then incubated at 37°C and 5% CO_2 for additional 30 min. and finally immersed in cell culture medium

1.6 Cell migration assay

Cell migration experiments were conducted at 37°C and 5% CO_2 and high relative humidity. Hydrogel discs containing dispersed cells were equilibrated for 4 hrs in cell culture medium and then 'glued' to the bottom of 24 well cell culture dishes by applying 10 μl of 5% hydrogel to the edge of the discs. After gelation was allowed to take place for 30 min, the samples were equilibrated for 1 hour in 1 ml of pure cell culture medium or medium that contained 50μM of the broad-range MMP inhibitor GM6001 (Chemicon). Three random (x-y-z) positions, carefully selected to be completely inside the matrix, were selected using an inverse wide-field microscope (Leica, DM IRBE) equipped with a motorized stage and focus, and a black and white camera (Hamamatsu ORKA ER). Cell spreading and migration was followed for up to 36 hours by software-controlled image acquisition (Openlab) every 15 minutes.

1.7 Statistical analysis of migration parameters

Projections of real 3D tracks were followed manually by using a "Manual Tracking" plugin in ImageJ software. The resulting x and y coordinates were used in a correlated random walk model, as described by Raeber et *al.* (17). This model assumes that the cell velocity decays exponentially with time with a characteristic time constant P (directional persistence time). Thus the mean-squared displacement of a cell during the time interval Δt is related to P and the root mean squared speed S by the equation which applies for cells migrating on 2D as well as in 3D:

$$<d^2(t)> = 2S^2P[t-P(1-e^{-t/P})] \quad (1)$$

Consistent with our earlier work, we observed no preferential migration direction when the distance was plotted against the direction in a polar plot (Fig. 3A and Supplemental Fig. 2) (17). Therefore for such isotropic migration, the projected cell speed S_{2D} was corrected by a geometry factor of sqrt(3/2) to give an estimate of S. The mean-squared displacements $<d^2(t)>$ from experimental cell-track data were calculated by the method of overlapping intervals and corrected to predict the 3D displacement from the 2D projections. The dimension-corrected cell speed S was used as an input parameter to fit Eq. 1 to the dimension-corrected displacement data by a nonlinear least-square regression analysis to obtain an estimate of the directional persistence time P. The persistence length L was defined as the product L = P x S. The S and P values of individual cell tracks from the same treatment and three independent experiments were pooled to generate cell-population histograms and box plots extending from the 25th to the 75th percentile, including the median, whiskers from the 10th to the 90th percentile, and a symbol corresponding to the arithmetic mean. Tracks with persistence time values derived from regression analysis with $R^2 \leq 0.6$ were excluded from the study. Homogeneity of variances and normality of errors was not given for migration parameters. For statistical analysis, multiple comparisons were therefore conducted with the Dunn's test, a nonparametric rank sum test suitable for unequal sample sizes. In an additional analysis the whole cell populations was divided, based on the persistence length criterion $L_{crit} \leq 1.2$ μm as a threshold, into a motile (persistence length $L \geq L_{crit}$) and a non-motile fraction. Since we were interested in cell motility in hydrogels with different compositions, this criterion allowed us to discriminate between cells that oscillated in cavities developed during the gelation process and cells that effectively migrate.

1.8 Staining and confocal microscopy

MC3T3-E1 cells were stained for f-actin and nuclei. Samples were fixed and permeabilized in 4% paraformaldehyde containing 0.2% Triton X-100 in PBS for 20 min at 4°C. Samples were incubated for 10 min in 0.1 M glycine followed by a wash step in PBS. For f-actin staining, the gels were incubated with 0.4 U/ml rhodamine-labeled phalloidin (R-415; Molecular Probes, Eugene, OR, USA) in PBS with 1% BSA for 1 h at 4°C. After washing the samples three times for 5 min in PBS, cell nuclei were co-stained with 1 ng/μl DAPI (4',6-diamidino-2-phenylindole) (D-1306; Molecular Probes, Eugene, OR, USA) in PBS for 10 min at 4°C. Z-series of approximately 30 equidistant x-y scans at 0.272 μm intervals (63x) were acquired and processed in Imaris software (Bitplane AG, Zürich, Switzerland).

For time-lapse confocal imaging, cells were stained with PKH-26 (Sigma-Aldrich) according to the manufacturer's instructions. Fluorescently labeled cells were encapsulated in hydrogels containing covalently linked TG-Lys-FITC (24). The resulting hydrogel discs were equilibrated

for 4hrs in cell culture medium and then glued to the bottom of 24 well cell culture dishes by applying 10 µl of 5% hydrogel to the edge of the discs. Z-series of approximately 100 equidistant x-y scans at 1.5 µm intervals (20x) were acquired for 8 hours at 15 min. intervals in resonant scanning mode with a Leica TCS SP5 confocal microscope and processed in Imaris software.

1.9 Animal experiments

Animal experiments were authorized by the Veterinary Authority of the Canton of Zurich. Adult female Sprague-Dawley albino rats (300-350 g) were used for bone regeneration experiments as previously described (25). Briefly, an 8 mm calvarial defect was created in the parietal bone with a dental handpiece. After removal of the calvarial disk, bone debris were removed by rinsing the surgical site. Preformed hydrogel disks (8 mm diameter and 1 mm in thickness) were placed into the defect. After two weeks, the animals were sacrificed and explanted skulls were fixed with 4% formalin before decalcification in Usedecalcâ~~Medite),~~ Nunningen, Switzerland). 5 mm paraffin sections were taken through the centre of the implantation site and, after staining with Hematoxylin and Eosin, composite images were generated with a 5x objective on a Leica DM 5500B microscope. For the quantitative evaluation of gel leftovers, images were superimposed onto a grid of 88 points/mm^2. The number of test points covering the remaining gel mass were counted and standardized against sections derived from gels that were not implanted. Four to five animals were used per gel type.